Mass and kinetic energy distributions in near-barrier fission of ^{182}W

B. D. Wilkins, B. B. Back, J. E. Gindler, and B. G. Glagola*
Chemistry Division, Argonne National Laboratory, Argonne, Illinois 60439

K. Kwiatkowski, S. H. Zhou,† and V. E. Viola, Jr.
Department of Chemistry and Cyclotron Facility, Indiana University, Bloomington, Indiana 47405
(Received 23 April 1984)

Mass and kinetic energy distributions have been measured for the fission of ^{182}W at an excitation energy above the fission barrier $E^*-E_f\approx 20$ MeV. A primary motivation for these studies was to search for evidence of asymmetric mass division and anomalously low total kinetic energy release, as predicted by scission-point model calculations which include deformed (Strutinsky) shell effects. Double kinetic energy measurements of coincident fission fragments were performed, from which fragment mass distributions were derived. From the data it is concluded that at this excitation energy, liquid-drop behavior dominates the fission of ^{182}W and any shell strength, if present, is less than 20 percent of full strength.

I. INTRODUCTION

Studies of nuclear fission at low excitation energies have demonstrated the important role of shell effects in determining fragment mass and kinetic energy distributions. It has been known that mass distributions at near-barrier energies exhibit a continuous transition from double humped for the fission of actinide nuclei to triple humped for radiumlike nuclei to a single symmetric peak in the lead region.[1] This behavior had been qualitatively explained in terms of the liquid-drop model, modified by spherical shell effects;[2–4] i.e., the energy stabilization provided by the $N=82$, $Z=50$ shell closures favors an asymmetric mass division for nuclei in the uranium region.

Subsequent models[5,6] have attempted to account for the characteristics of the fission process more quantitatively by the inclusion of deformed shell effects. The scission-point model,[6] a static model which assumes statistical equilibration among the collective degrees of freedom at the scission point, has been successful in explaining many of the observed fission phenomena. In this model the total potential energy of the system at the scission point is calculated as the sum of liquid-drop, shell, and pairing terms with Coulomb and nuclear potential terms describing the interaction between the fragments. A key feature of this model is the inclusion of deformed shell effects in the fragment potential-energy surface, following the Strutinsky prescription.[7] This model has proven successful in providing a much more comprehensive description of fission mass and kinetic energy distributions and the dependence of these upon excitation energy. Particularly important in these calculations is the influence of fragment deformation in determining the fragment kinetic energy distributions. An important early prediction of this model was that the neutron-excess isotopes of fermium ($Z=100$) would exhibit symmetric mass division and an anomalously high total kinetic energy release due to the influence of closed spherical shells at $Z=50$ and $N=82$. This behavior is observed in the spontaneous fission of ^{258}Fm and ^{259}Fm.[8,9]

The scission-point model of Ref. 6 also predicts the existence of mass regions below $A=200$, where asymmetric mass division may be competitive with symmetric fission, which is predicted by the liquid-drop model. One such region occurs in the vicinity of the nuclide $^{182}_{74}W_{108}$. For deformations near $\beta\approx 0.55$ strong minima in the potential-energy surface are calculated for $N=64$ and 44 and for $Z=44$ and 30. These minima present a very favorable situation for asymmetric fission, for the complementary fragments would have both N and Z shells at the *same* deformation and N-to-Z ratios which are nearly the same as the ratio in the fissioning nucleus, 1.46. Thus, on the basis of the scission-point model, the fission of ^{182}W with zero excitation energy is predicted to form a mass split of $A_H=108$ ($Z_H=44$, $N_H=64$) and $A_L=74$ ($Z_L=30$, $N_L=44$) with a β deformation of ~ 0.55 for both fragments. Because the total deformation ($\beta_L+\beta_H\approx 1.10$) for this mass split is larger than that predicted on the basis of the liquid-drop model, the total kinetic energy for this split is expected to be anomalously low.

A second asymmetric fission configuration is possible for ^{182}W in which there are strong N and Z shell effects at the same β deformation and the N-to-Z ratio in the two fragments is nearly the same as that of the fissioning nucleus. This configuration of $A_H=98$ ($Z_H=40$, $N_H=58$, $\beta_H=0.4$) and $A_L=84$ ($Z_L=34$, $N_L=50$, $\beta_L=0.1$) would be expected to have a relatively high total kinetic energy release, as the total deformation of this configuration is much less than that expected from liquid-drop forces. Therefore, observation of mass asymmetry and structure in the total kinetic energy release as a function of fragment mass for the fission of nuclides in the region of ^{182}W would serve to further reinforce the predictive power of the scission-point model. However, in order to detect these effects, experiments must be performed at sufficiently low excitation energy for the shell effects to be competitive with symmetric fission, which is

favored on the basis of liquid-drop forces. To date no such experiments have been performed because of the very low cross sections in the near-barrier region for nuclei well below the lead region.

II. EXPERIMENTAL PROCEDURE

In these studies the reaction

$$^4\text{He}+^{178}\text{Hf}\rightarrow^{182}\text{W}^*\rightarrow\text{fission}$$

was studied with 49.2-MeV ^{4}He ions from the Indiana University Cyclotron Facility (IUCF). Beam intensities were typically 200—400 nA. For the formation of ^{182}W, $Q=-1.7$ MeV and the liquid-drop fission barrier[10] for ^{182}W at $l=0$ is 26.3 MeV. Thus, the excitation energy of the fissioning nuclei prepared in this system is $E^*-E_f\geq 20$ MeV, depending on angular momentum. Fission of nuclei with $A\leq 210$ in this energy region is known to be dominated by complete fusion processes,[11] and must be primarily first-chance fission because of the very strong dependence of the fission cross section on excitation energy in the barrier region. The bombarding energy of 49 MeV was chosen as a compromise between the demands of low excitation energy in order to preserve significant shell strength in the fissioning nucleus and those imposed by cross section, measured[12] to be about 2 μb for this system at 49 MeV.

An isotopically separated ^{178}Hf target of thickness ≈ 100 μg/cm^2 was prepared in an isotope separator on a 60-μg/cm^2 carbon foil. Although actinide contamination was only about one part in 10^7, this was sufficient to make a noticeable contribution to the observed fission spectrum. Actinide fission was partially eliminated by means of procedures described in the following section. Fission coincidence events were detected with three pairs of silicon surface-barrier semiconductor detectors, each of area 400 mm^2 and a nominal depletion depth ≈ 100 μm, placed inside the 162-cm-diam scattering chamber at IUCF. Each detector pair was mounted in a coplanar configuration which included the beam axis and target center. Within this plane the angle between each detector pair, θ_{AB}, was defined by the constraints of complete fusion kinematics leading to symmetric binary fission, i.e., $\theta_{AB}=170°$. The three coincidence planes thus defined were arranged so that the azimuthal angle Φ between each plane was $\Phi=0°$ and $\pm 30°$ with respect to the horizontal plane of the scattering chamber. One detector of each pair was placed 7.5 cm from the target and the other detector at 10.2 cm. This arrangement was a compromise to provide a reasonably large solid angle, to ensure that the fragments which were counted in the more distant detector would have their complements counted in the closer detector (detector efficiency), and to give measurable timing differences in the flight paths. The latter were used in analyzing the data as described below.

Fragment energies were determined from coincident events, with fast-timing coincidence circuitry based on fast-timing pickoffs of the Sherman-Roddick-Metz design.[13] Detectors were calibrated with a ^{252}Cf source using the calibration scheme of Kaufman *et al.*[14] Fragment energy resolution was approximately ± 2 MeV. Masses were then determined according to the double-energy technique assuming (1) complete fusion kinematics, (2) binary fission of ^{182}W only, and (3) neutron emission from the fragments as calculated from the available excitation energy and $\langle E_n\rangle=2T$, where $T=\sqrt{E^*/a}$ with $a=A/8$ MeV^{-1}. Folding in the uncertainties in fragment energies, kinematics (due to the large solid angles), and neutron evaporation energetics, we estimate a final mass resolution of ± 4 u. This resolution was considered sufficiently accurate to distinguish between a symmetric mass split and one with $A_H/A_L=108/74$. Crude masses were also calculated by means of the fast-timing information obtained in these measurements. These masses were compared with those calculated from energy measurements. Events which gave inconsistent results were discarded.

Approximately 2100 valid coincidence events were observed during the course of these experiments. Of these, about 12% were attributed to actinide fission. Of the remaining 1850 events, it was estimated that less than 3% of these could be due to heavy-element fission.

III. RESULTS

In Fig. 1 a two-dimensional contour plot of the center-of-mass E_1 vs E_2 distribution is shown for all valid coincidence events observed in these experiments. The contribution of high-energy actinide fission to the total distribution is apparent in the portion of the data with large E_1 and E_2 values. In order to eliminate these spurious events, a window was set on the data (dashed line in Fig. 1) for which it was assumed that

$$E_K=\frac{Z_L Z_H e^2}{r_0(A_L^{1/3}+A_H^{1/3})}=kA_L A_H\ . \tag{1}$$

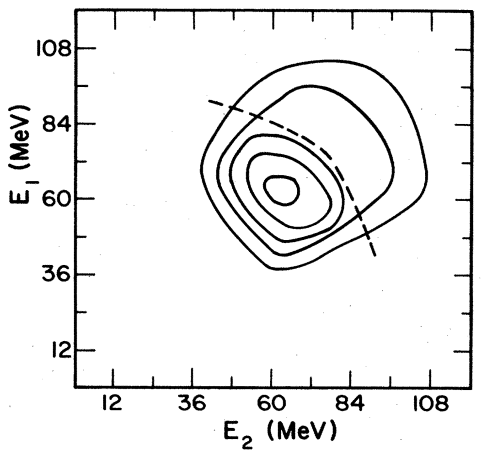

FIG. 1. Contour plot of center-of-mass, preneutron evaporation fragment kinetic energies, E_1 vs E_2, for the fission of ^{182}W. Each solid line represents a contour representing a factor of 2 in relative cross section. The dashed line represents the window defined by Eq. (1) (see the text), above which all events were eliminated from the data analysis.

For symmetric fission E_K was taken to be 150 MeV and Eq. (1) was solved for k. This value of k was then used to determine the window shown in Fig. 1 for all fission events. Events with values in excess of this window ($\sim 12\%$) were eliminated from the data set in subsequent analysis. It is estimated that the remaining fission coincidences contain about a 3% contamination due to actinide fission. This value was obtained by assuming ^{238}U(^{4}He,f) to be the contaminant and estimating from $E_K(A)$ and $\sigma_{E_K}(A)$ the percentage of fission events that fall below the dashed line of Fig. 1. A similar percentage of valid coincidences from ^{182}W fission is probably eliminated by this method. All additional data (Figs. 2—5) include only events which have passed the above-mentioned software window.

In Fig. 2 the mass distribution determined for ^{182}W fission, corrected for neutron emission, is shown. Error bars include only statistics. The solid line in Fig. 2 represents a Gaussian function that has been constrained to fit the symmetric and far-asymmetric regions of the mass distribution in order to accentuate any possible shoulder in the $A=100$—108 region of the curve. Although a weak deviation in the mass yield curve above the Gaussian fit is observed in this region, the evidence for a definitive mass asymmetry effect is not compelling. From these data the standard deviation of the mass distribution is determined to be $\sigma=9.0$ u.

The experimental total kinetic energy release E_K and variances in E_K are shown in Figs. 3(a) and (b), respectively, as a function of heavy fragment mass, A_H. From these data a most probable E_K value of $\langle E_K \rangle = 128.6$ MeV is obtained with an estimated error of ± 2 MeV. This value is in good agreement with $\langle E_K \rangle = 125.6$ MeV, based on systematics.[15] The standard deviation for the E_K distribution is 9.4 MeV. The dashed curve in Fig. 3(a) is the liquid-drop expectation for the dependence of E_K on fragment mass, as given by the scission-point model of Ref. 6 with all shell strengths set equal to zero. The neck length d in the calculations [Eq. (1)] has been adjusted to fit the E_K systematics of Ref. 15. The most probable total kinetic energy release from the model is then obtained by taking the calculated E_K at each mass split and weighting it with the experimental mass yield. In the region $A_H \sim 102$—108 [Fig. 3(a)] the value of E_K deviates slightly above the E_K curve. Again, the effect is not distinct, and furthermore, it should be noted that deviations above liquid-drop behavior indicate enhanced sphericity for the fragments, rather than more deformed shapes. Hence, if the observed weak deviation is real, it would imply that the neutron shell at $N=50$ ($\beta=0.1$) and at $N=58$ ($\beta=0.4$) is responsible. However, it should be remembered that a few percent of the "valid" events may be the result of actinide fission. Assuming that the actinide contaminant is ^{238}U, the most probable mass splits[16] for the reaction ^{238}U + ^{4}He are $A_H=138$—142 and $A_L=104$—100. If these most probable actinide fission events are assumed incorrectly to be ^{182}W fission events, the mass splits calculated will be $A_H=104$—107 and $A_L=78$—75, just where the deviations appear in Fig. 3. It is therefore possible that the observed deviations are caused by spurious actinide fission events that have not been completely eliminated in analysis.

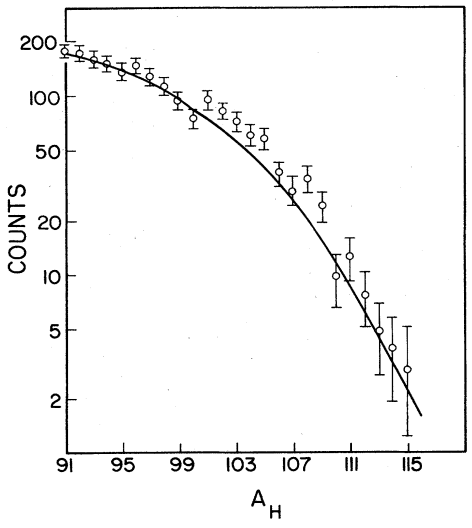

FIG. 2. Relative mass yield curve for fission of ^{182}W at $E^*-E_f \approx 20$ MeV. Solid line is a Gaussian function fit to the symmetric and far asymmetric regions of the distribution.

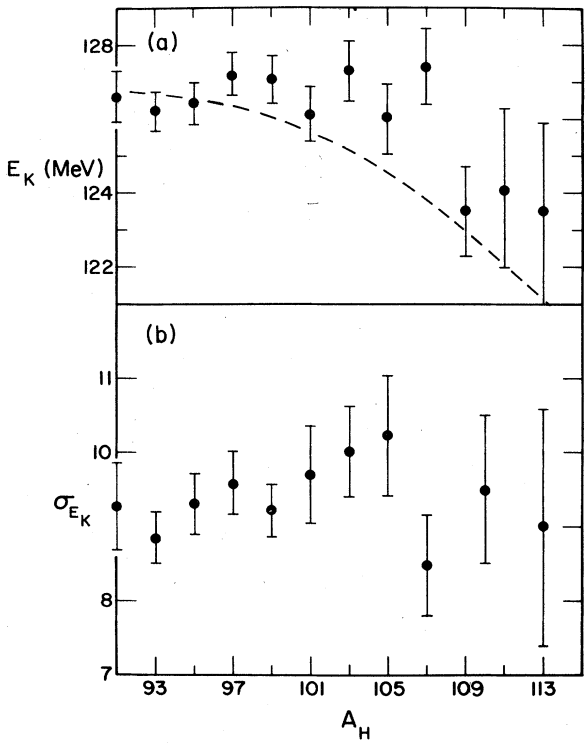

FIG. 3. Total kinetic energy release (a) and standard deviation in E_K (b) as a function of heavy fragment mass, A_H, for fission of ^{182}W.

Figures 4 and 5 show the predictions of the scission-point model[6] for fission of ^{182}W for the relative mass yield and E_K distributions for various shell strengths, using the same assumptions concerning the neck length d and $\langle E_K \rangle$ from systematics,[15] as above. The data are best fit by the liquid-drop calculation (shell strength=0.0) and cannot tolerate any shell strength greater than 0.2. On the basis of this analysis we conclude that liquid-drop behavior dominates the fission of ^{182}W at this excitation energy and that any shell strength, if present, is $\leq 20\%$ full strength.

The fact that no definitive evidence for shell effects is observed in the fission of ^{182}W at $E^* - E_f \simeq 20$ MeV must be examined in the context of evidence for shell effects in the fission of thorium or uranium at 20–30 MeV above the fission barrier.[17] The mass distributions for these latter fissioning systems are slightly asymmetric in character, which is accounted for in the scission-point model[6] as due to the effect of shells. In fact, it was because of these distributions that the present experiment with ^{182}W was attempted. There are, however, at least two major differences between the fission of a lower-Z nucleus, such as ^{182}W, and a uranium or plutonium (Th + ^{4}He or U + ^{4}He) nucleus excited to 20 MeV above E_f. The excited lower-Z nucleus has essentially only one chance to fission. That is, it either fissions or emits a neutron, after which the excitation energy is so low ($\sim$10 MeV $> E_f$) that the probability for the resulting A-1 nucleus (e.g., ^{181}W) to fission is negligible. This is not the case for the fission of an actinide system in which second- and third-chance fission are appreciable. Vandenbosch *et al.*[18] have estimated that the interaction of 32-MeV ^{4}He ions with ^{235}U, which results in a ^{239}Pu* nucleus with $E^* - E_f \approx 20$ MeV (nearly the same as in the present case of ^{182}W), yields 78% first-chance, 16% second-chance, and 6% third-chance fission. It is therefore possible that the structure observed in the mass distributions of the actinides is caused entirely by contributions from second- and third-chance fission which occur at significantly lower excitation energy. An attempt by the present authors to extract a first-chance fission mass distribution for the 32-MeV ^{4}He-ion-induced fission of ^{235}U from the data of Vandenbosch *et al.*[18] gave results sufficiently crude as to preclude any definitive statement about the shape of the mass distribution.

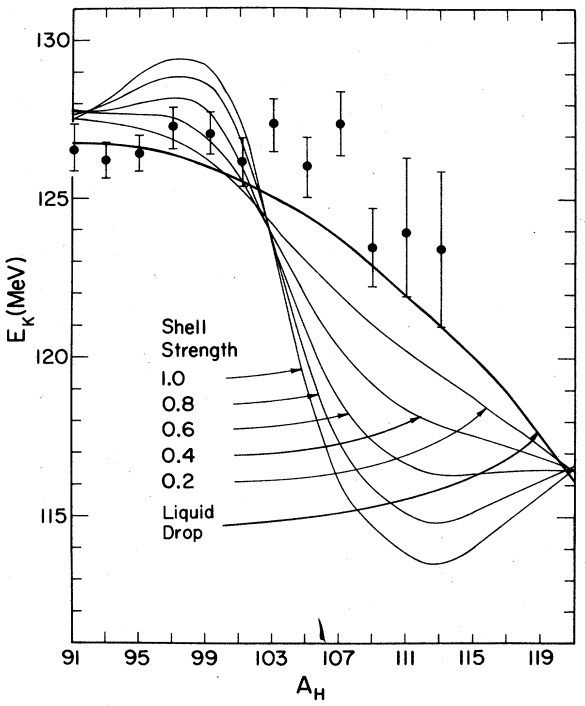

FIG. 5. E_K data as a function of heavy fragment mass, A_H, for fission of ^{182}W. Solid lines compare predictions of the scission-point model (Ref. 6) for various shell strengths, as indicated in the figure.

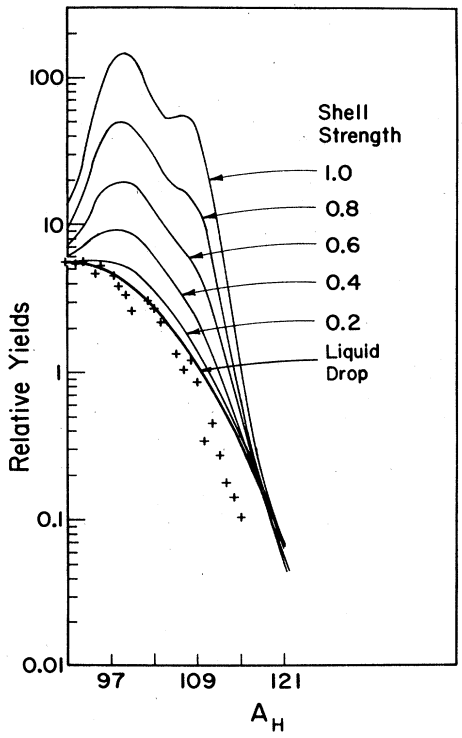

FIG. 4. Relative mass yield curve (x) for fission of ^{182}W. Solid lines compare predictions of the scission-point model (Ref. 6) for various shell strengths, as indicated in the figure.

The second major difference between ^{182}W fission and actinide fission concerns differences in shapes between the saddle and scission points. For a high-Z system in the actinide region the saddle configuration is relatively compact with a thick neck between nascent fragments. The descent to the elongated, narrow-necked scission configuration not only involves a significant decrease in potential energy with the possible interplay of fission dynamics, but must also require a relatively long time for the nucleus to adjust to these large changes in energy and shape. This time would allow the system to adjust to any microscopic shell effects. However, for a light-Z system, such as ^{182}W, the saddle and scission configurations are essentially

the same. Thus, very little time is needed to scission after the saddle point is achieved. For such a system excited to 20 MeV above the fission barrier it is conceivable that there is insufficient time for any expected shell effects to express themselves at scission. It is noteworthy that just where the calculated saddle and scission points approach each other (i.e., the Pb region), any shell effects which can be observed experimentally disappear.

In order to conduct a more conclusive test of the prediction of deformed-shell effects in the fission of ^{182}W, or neighboring nuclides for which the effects may be more dominant, it would appear that fission at substantially lower values of E^*-E_f must be explored. This is a very difficult and time-consuming experiment with present-day accelerator and detector technologies. Nonetheless, these data do constitute a test of liquid-drop mass and kinetic energy properties of $A \leq 200$ nuclei at the lowest excitation energy yet studied. As such, they provide a useful confirmation of the underlying liquid-drop properties of nuclear matter.

ACKNOWLEDGMENTS

The authors wish to recognize the contribution of J. Lerner (deceased) of Argonne National Laboratory, who prepared the ^{178}Hf targets. The assistance of Terry Sloan of IUCF in constructing the detector mounts was also appreciated. In addition, we acknowledge Dennis Freisel and the IUCF machine operations crew for excellent beams during these experiments. This work was performed under the auspices of the Office of High Energy and Nuclear Physics, Division of Nuclear Physics, U.S. Department of Energy under Contract Nos. W-31-109-ENG-38 and DE-AC02-81ER-40007, and the National Science Foundation.

---

*Present address: U.S. Naval Research Laboratory, Washington, D.C. 20375.

†Present address: Institute of Atomic Energy, Academica Sinica, Beijing, People's Republic of China.

[1]R. Vandenbosch and J. R. Huizenga, *Nuclear Fission* (Academic, New York, 1973).

[2]R. Vandenbosch, Nucl. Phys. **46**, 129 (1963).

[3]J. Terrell, Phys. Rev. **127**, 880 (1962).

[4]H. W. Schmitt, *Proceedings of the 2nd International Symposium on Physics and Chemistry of Fission* (IAEA, Vienna, 1969), p. 69.

[5]U. Mosel and H. W. Schmitt, Phys. Rev. C **4**, 2185 (1971).

[6]B. D. Wilkins, E. P. Steinberg, and R. R. Chasman, Phys. Rev. C **14**, 1832 (1976).

[7]V. M. Strutinsky, Nucl. Phys. **A95**, 420 (1967).

[8]E. K. Hulet, R. W. Lougheed, J. H. Landrum, J. F. Wild, D. C. Hoffman, J. Weber, and J. B. Wilhelmy, Phys. Rev. C **21**, 966 (1980).

[9]D. C. Hoffman, J. B. Wilhelmy, J. Weber, W. R. Daniels, E. K. Hulet, R. W. Lougheed, J. H. Landrum, J. F. Wild, and R. J. Dupzyk, Phys. Rev. C **21**, 972 (1980).

[10]W. D. Myers and W. J. Swiatecki, Nucl. Phys. **81**, 1 (1966); W. D. Myers and W. J. Swiatecki, Lawrence Berkeley Radiation Laboratory Report UCRL-11980, 1965.

[11]W. G. Meyer, V. E. Viola, Jr., R. G. Clark, and S. M. Read, Phys. Rev. C **20**, 176 (1979).

[12]A. Khodai-Japoori, Lawrence Berkeley Radiation Laboratory Report UCRL-16489, 1966.

[13]I. S. Sherman, R. G. Roddick, and A. F. Metz, IEEE. Trans. Nucl. Sci. **15**, 500 (1968).

[14]S. B. Kaufman, B. D. Wilkins, and E. P. Steinberg, Nucl. Instrum. Methods **115**, 47 (1974).

[15]V. E. Viola, Jr., At. Data Nucl. Data Tables **1**, 391 (1966).

[16]J. P. Unik and J. R. Huizenga, Phys. Rev. **134**, B90 (1964).

[17]E. K. Hyde, *The Nuclear Properties of the Heavy Elements. III. Fission Phenomena* (Prentice-Hall, Englewood Cliffs, N.J., 1964).

[18]R. Vandenbosch, T. D. Thomas, S. E. Vandenbosch, R. A. Glass, and G. T. Seaborg, Phys. Rev. **111**, 1358 (1958).